Optics Communications 284 (2011) 4073–4077

Contents lists available at ScienceDirect

Optics Communications

journal homepage: www.elsevier.com/locate/optcom

Ring resonator of surface modes based on photonic crystals

Hongliang Ren [a], Jinghong Zhang [a,*], Yali Qin [a], Kai Liu [a], Zhefu Wu [a], Weisheng Hu [b], Chun Jiang [b], Yaohui Jin [b]

[a] College of Information Engineering, Zhejiang University of Technology, Hangzhou 310023, China
[b] State Key Laboratory of Advanced Optical Communication Systems and Networks, Shanghai Jiao Tong University, Shanghai 200240, China

ARTICLE INFO

Article history:
Received 30 August 2010
Received in revised form 30 March 2011
Accepted 1 April 2011
Available online 21 April 2011

Keywords:
Circular photonic crystal (CPC)
Surface mode waveguide (SMW)
Surface mode ring waveguide (SMRW)
Ring resonator

ABSTRACT

We design a compact ring resonator of surface modes based on photonic crystals (PCs). The structure is formed by sandwiching a surface mode ring waveguide (SMRW) into two parallel surface mode waveguide (SMW) based on two dimensional (2D) PCs. The SMRW is created on the surface of a circular photonic crystal (CPC) structure, where the wave propagates with high transmission efficiency. As a fundamental mode is introduced in the input SMW, at certain frequencies, the SMRW modes are enhanced because of resonance and the light-waves are coupled to the output SMW. It is demonstrated by the simulation results that the surface mode ring resonator has a low radiation loss with a very small size because of the good wave-guiding of surface mode based on PCs, and can be used in the future wavelength division multiplex (WDM) optics communication systems.

1. Introduction

Optical waveguide ring resonators can be utilized as channel drop filters, which are very crucial components for WDM optic communication systems, photonic integrated circuits, and optical computing [1–7]. In order to make use of the precious bandwidth resource, the free spectral range (FSR) of the resonators is increased regularly and remarkably by reducing the ring radius directly. However, in the strip-based SOI ring resonator, the radiation loss increases exponentially with reduction of the ring radius, so the minimum of the ring radius is about 3 μm in this case [4–7]. To reduce the radius of ring and achieve a larger FSR, a photonic crystal ring resonator is proposed by Qiang.et al. [8]. The ring resonators are composed by the line-defect waveguide in the interior PCs with square lattice, but it is very difficult to build the device based on PCs with hexangular lattice due to the great propagation loss at the corner of the ring resonators [8–12]. Recently, it has been suggested that PCs surface waveguide can realize light-waves transmission with high efficiency [13,14]. A photonic crystal surface waveguide is created on the surface of a circular photonic crystal (CPC) structure, which is formed by removing a concentric layer from the CPC [14]. The curve waveguide can realize high power transmission because of its smoother bend with smaller discontinuity and the symmetry about the center of the curve waveguide. Compared to line-defect waveguide in the conventional PC with hexangular lattice, it is easier to make use of the curve waveguide to build a photonic crystal ring resonator.

In this paper, a surface mode ring resonator based on hexagonal lattice PCs is proposed. The symmetrical resonant filter is formed by sandwiching one SMRW into two parallel SMWs. The SMWs are obtained by increasing the radii of the row of rods between the hexangular lattice dielectric PCs and air. The SMRW is created on the surface of a CPC structure by increasing the radii of the rods at the outmost concentric circumference. The device is calculated by the finite difference time domain (FDTD) method with the perfectly matched layer absorbing boundary conditions at all boundaries. Compared with other surface mode ring resonators [3], the ring resonant structure based on PCs with hexagonal lattice has a very low energy loss, and most of the light in the input waveguide can be transferred to the output waveguide at resonance. The device with simple structure provides a possibility of channel drop filter, and can be used in future WDM optic communication systems or other fields.

2. Design of the ring resonance

We consider a semi-infinite hexangular lattice PCs composed of cylinders with $\varepsilon = 11.6964$ and a diameter of $D_b = 0.392a$ in an air background, where a is the lattice constant. As shown in Fig. 1(a), the surface geometries is researched, supporting the surface states, where the outermost surface rods have increased their diameters $D = 0.5a$, and the distance between two nearest-neighbor surface rods satisfies $d = 0.5a$. For effective localization of electromagnetic light-waves on the PC surface, two conditions must be met: the surface mode must be in the PBG and only the part of surface mode that lies below the light-line is taken into account [13]. The hexagonal PCs have a fundamental band-gap for TM polarization in the frequency range of $0.28481(c/a) < f < 0.4557(c/a)$ and supports two surface modes below the light-line

* Corresponding author.
E-mail address: zhangjinghong@zjut.edu.cn (J. Zhang).

0030-4018/$ – see front matter © 2011 Elsevier B.V. All rights reserved.
doi:10.1016/j.optcom.2011.04.003

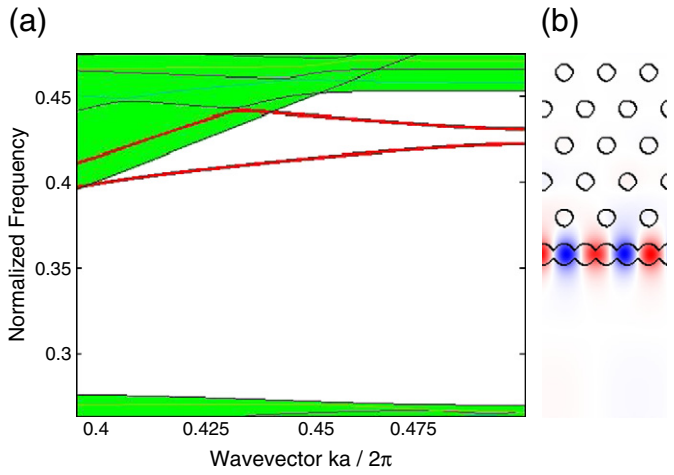

Fig. 1. (a) Band structures for TM modes PCs with the hexangular lattice composed of rod diameters $D_b = 0.392a$ and permittivity $\varepsilon = 11.6964$ along with the projected surface modes. The diameters of the surface rods are $D = 0.5a$, and the distance between two nearest-neighbor surface rods is $d = 0.5a$. (b) The normalized intensity of the E_z components of surface-mode dispersion curves.

for the case of Fig. 1(a), where λ is the wavelength of light in the free space. For the structure of Fig. 1(b), the field intensity has one maximum with each rod and extends into the air, quickly decaying into the crystal with a width of a. For the case of the structure of Fig. 1 (b) with enlarged surface rods, the intensity of both surface modes is mainly localized within the surface rods and its extent to the air is small for the whole energy range [14].

For conventional line-defect curve waveguide in PCs [13], light-waves are controlled on both side of the waveguide by the photonic band-gap, which act like a Bragg reflecting curve mirror. However, the SMRW has only a periodic structure on one side of the waveguide. Light-waves traveling around the SMRW have to change their magnitude and direction vectors. The large concentric distance and small bending radius of the SMRW lead to the abrupt change of magnitude and direction vector of the wave-vector. So the light-waves can radiate to the surrounding air background easily. One way to reduce this radiation loss is to reduce the surface concentric distance d_c, and then the waveguide has high overall surface effective index and high confinement factor. Fig. 2(a) shows half the SMRW, which is formed at the outermost concentric layer (i.e., $N = 8$) by increasing the radius of the surface rods to $0.25a$, where the distance d_c between the nearest-neighbor surface rods at the outermost layer is $0.4887a$. Fig. 2(b) shows that high power transmissions for half the SMRWs, and the transmission spectra at $d_c = 0.4887a$ and $d_c = 0.6109a$ are denoted by the thick and thin solid lines, respectively. The former transmission efficiency is higher than that in the latter for the interest frequency range. It indicates that the SMRW has high power transmission efficiency with a high surface effective index due to a large radius of the rods on the surface and a little distance d_c between the nearest-neighbor surface rods.

So the designed SMWs are utilized as two parallel waveguides in the symmetric resonant systems as shown in Fig. 3(a). The structure is formed by sandwiching one SMRW into two parallel SMWs. The SMRW is created on the surface of a CPC structure. Fig. 3(a) shows the 2D CPC structure with circular cylindrical rods diameters of $0.392a$, and these rods has permittivity of 11.6964, which parameters are completely same to that of the above-mentioned PCs with hexagonal lattice. The CPC structure has radial periodicity, and the distance between each concentric layer is constant, where it is a. The structure has a six-fold symmetry and the number of rods in each layer is given by the formula $6(N\text{-}1)$, where N denotes the number of layer with $N \geq 2$. A SMRW is formed by removing a concentric layer from the CPC. Here, a ring waveguide is formed at the outermost concentric layer (i.e., $N = 8$) by increasing the radius of the surface rods to $0.25a$, where the distance d_c between the nearest-neighbor surface rods at the outermost layer is $0.4887a$, as shown in Fig. 3(a).

As shown in Fig. 3(a), the symmetrical resonant filter based on PCs is designed. The resonant structure is formed by sandwiching one SMRW into two parallel SMWs. The ring resonator is realized by the SMRW, and two parallel SMWs are used as the input and output waveguides, respectively. To realize modes match between the SMWs and SMRW, two main methods are considered: one is that the corresponding parameters between the hexagonal lattice PCs and CPC structure is same, including that the lattice constant is equal to the distance between each concentric layer and their background circular cylinder rods have the same radius and refractive index, and it is possible that the match between SMWs and SMRW modes is achieved based on the similar lattice structure. The other depends on the design of the SMWs and SMRW, including that these surface rods have the same radius and the distances between the nearest-neighbor surface rods are approximately equal. In the case, the distances are $0.5a$ and $0.4887a$ for the SMWs and SMRW, respectively. It is easily understood that the similar surface mode waveguide designs reduce the modes mismatch conveniently.

In the resonant structure, the waveguide/ring distance is the same crucial parameters as that for the traditional resonant micro-ring. The resonant filters with high efficiency will not be realized for the improper value of the waveguide/ring gaps. As shown in Fig. 3(a), the gaps between the SMWs and SMRW are denoted as g_u and g_b,

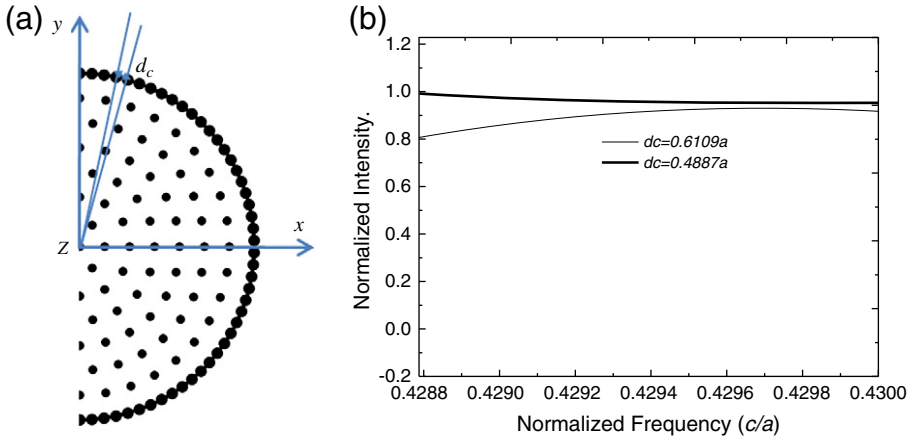

Fig. 2. (a) Schematic layout of CPC lattice structure with half the SMRW. (b) Transmission spectrum for half the SMRW at $d_c = 0.4887a$ (thick solid line) and $d_c = 0.6109a$ (thin solid line).

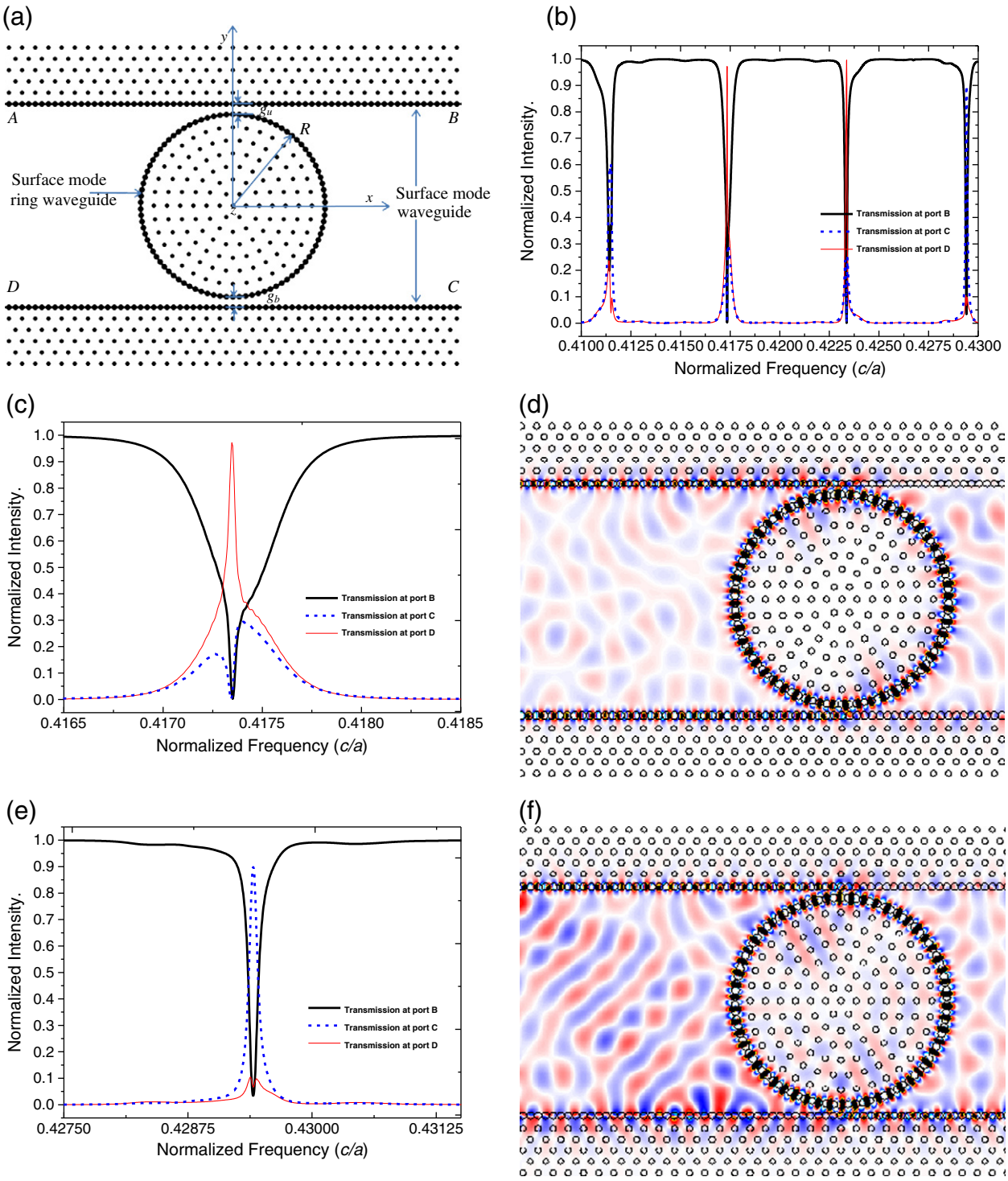

Fig. 3. (a) The schematic diagram of the ring resonator by sandwiching one SMRW into two parallel SMWs based on 2D PCs with the hexagonal lattice at $R=7a$. (b) Power transmission spectra at port B, C and D as the light is launched at the port A of the input waveguide. (c) Power transmission spectra at $0.4165(c/a)<f<0.4185(c/a)$. (d) Electric field distributions in the resonant ring at the normalized frequency $f=0.41735(c/a)$. (e) Power transmission spectra at $0.4275(c/a)<f<0.43125(c/a)$. (f) Electric field distributions in the resonant ring at the normalized frequency $f=0.4294(c/a)$. The parameters labeled in Fig. 2(a) are given as $R=7a$, $D=0.5a$, $d=0.5a$, $d_c=0.4887a$ and $g_u=g_b=0.734a$.

respectively. Here, $g_u=g_b=0.734a$. It is worth noting that it is necessary to place the surface rods carefully in coupling region between SMWs and SMRW. The centers of both proximal rods between the SMWs and SMRW must be on the y axis, otherwise a good coupling between the SMWs mode and SMRW mode will not be acquired. The reason is possibly that the positions of two surface mode nodes are corresponding with each other in coupling region so that their coupling occurs well.

When a fundamental TM mode (Electric field is perpendicular to x–y plane) is introduced in the input waveguide, it will be coupled to the SMRW, and excites surface mode based on these surface rods in the outermost concentric circumference. At certain frequencies, the

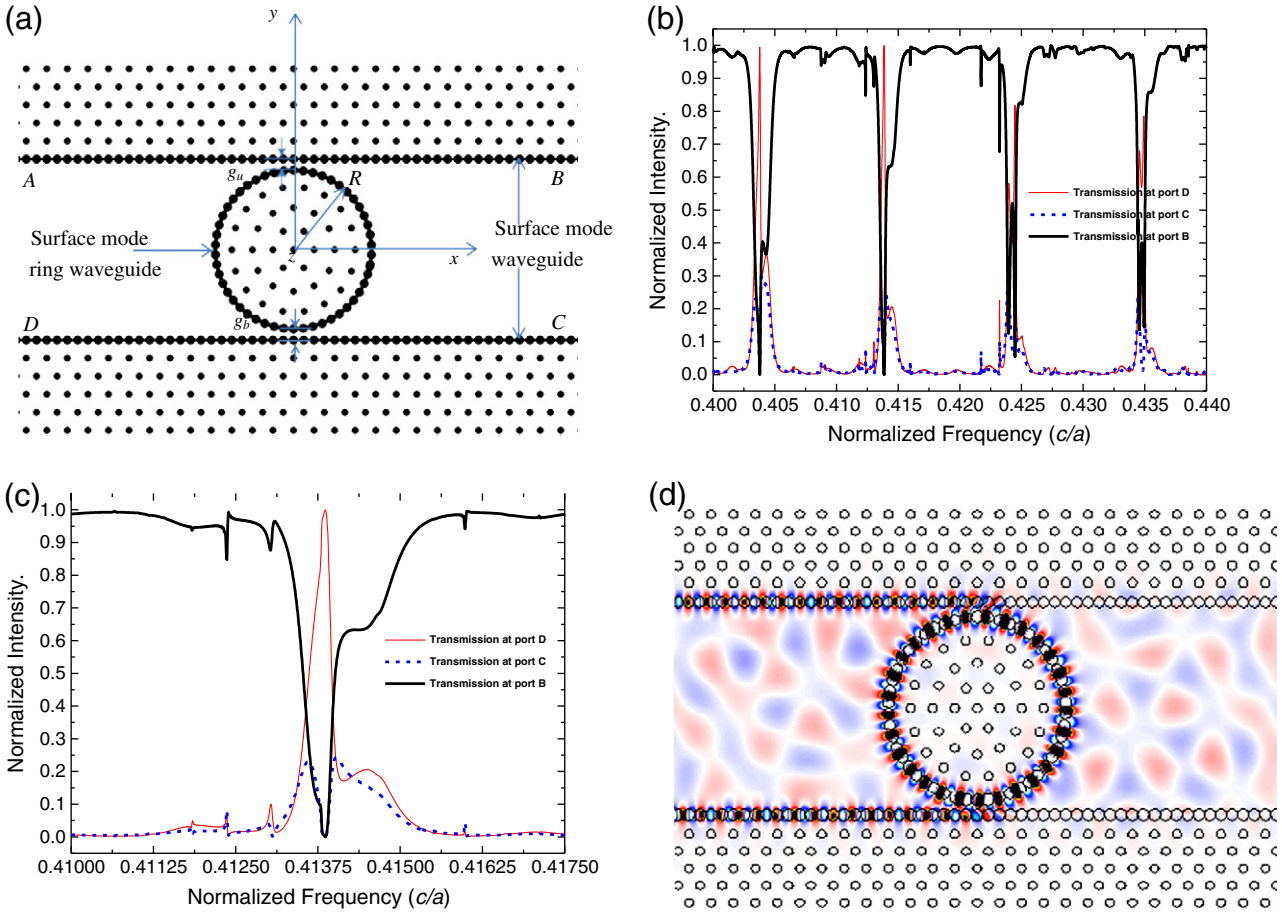

Fig. 4. (a) The schematic diagram of the ring resonator at $R=4a$. (b) Power transmission spectra at port B, C and D at $R=4a$. (c) Power transmission spectra at $0.41(c/a)<f<0.4175(c/a)$. (d) Electric field distributions in the resonant ring at the normalized frequency $f=0.41386(c/a)$. The parameters labeled in Fig. 3(a) are given as $R=4a$, $D=0.5a$, $d=0.5a$, $d_c=0.5027a$ and $g_u=g_b=0.644a$.

surface modes will be enhanced in the SMRW because of resonance and then the power is transferred to the output waveguide. FSR (free spectral range) of the ring can be obtained from the following equation:

$$FSR=\frac{c}{2\pi n_{eff}R} \tag{1}$$

where c is the light velocity in air, n_{eff} is the effective refractive index of the ring and R is its radius.

As the light is launched at the port A in Fig. 3(a), three time monitors for the transmission light-waves energy is set at the port B, C and D, respectively. Then, the designed device is calculated by the FDTD method with the perfectly matched layer absorbing boundary conditions at all boundaries. The normalized power transmission spectra are obtained by considering the sum of powers at port B, C and D as the total input power. Fig. 3(b) depicts the transmission spectra of the ring resonator for the ring radius $R=7a$, where the power transmission at port B, C and D are denoted as the thick solid, dot dashed, and thin solid curves, respectively. At resonant frequencies, most of the power is transferred from the input waveguide to the output one through the resonant ring. The values of FSR are usually achieved from the transmission spectra of the ring resonator. FSR is namely the frequency interval between two neighbor resonant peaks, where it is $0.00602(c/a)$. So the effective refractive index of the ring n_{eff} is 3.7768 according to Eq. (1).

Fig. 3(c) describes the Power transmission spectra at $0.4165(c/a)<f<0.4185(c/a)$. It is clear that the dropping spectrum at port D is not still Lorentz line shape, which maybe results from the mismatch between SMW and SMRW modes. The resonators have a quality factor around 6474, which is not much higher than the results of other type of ring resonators, and the radius of the ring resonator can be increased to improve its quality factor. Fig. 3(d) illustrates the electric field distribution in the ring resonator for the ring radius $R=7a$ at $f=0.41735(c/a)$. When the input waveguide is excited at the port A by a light-wave at $f=0.41735(c/a)$, the resonance occurs in the SMRW and most of the power is transferred to the output waveguide. One can see that electromagnetic field in the SMRW is strongly enhanced at the resonant frequency. However, there are a little light being radiating to the surrounding air background as the resonance occurs, which results from the little radiation loss of these surface mode waveguides. These light-waves being radiating is reflected back and forth between two parallel SMWs, and then there is a little power distribution in the air background between two parallel waveguides from the Fig. 3(d).

The transmission spectra at $0.4275(c/a)<f<0.43125(c/a)$ is shown in Fig. 3(e). It is interesting that the forward dropping at the port C predominates at $f=0.4294(c/a)$, which is obviously different with the dominance of backward dropping at resonance for the traditional resonant single micro-ring structure. The forward dropping is enhanced at certain frequencies, and the particular mechanism is not understood so far. In this case, the incident wave at port A only generates the resonant mode with clockwise traveling, and there is no direct coupling between incident wave and another counter-clockwise traveling mode [15]. However, the clockwise and counter-clockwise traveling resonant modes are related by the mutual

coupling. So the counter-clockwise resonant mode is improved due to both resonant modes coupling, and then most light-waves are forward dropped at the port C. Fig.3(f) illustrates the electric field distribution in the ring resonator for the ring radius $R=7a$ at $f=0.4294(c/a)$.

Fig. 4(a) shows the schematic diagram of the symmetrical resonator at $R=4a$, where the distance between the nearest-neighbor surface rods at the outermost layer is adjusted to $d_c=0.5027a$ and the SMRW/SMW distance is changed to $g_u=g_b=0.644a$. Fig. 4(b) shows the transmission spectra at port B, C and D, which are donated by the thick solid, dot dashed and thin solid curves, respectively. It is clear that FSR is $0.01(c/a)$ from the Fig. 4(b), and then the effective refractive index $n_{eff}=3.979$ for the SMRW. In Fig. 4(c), the transmission characteristics at $0.41(c/a)<f<0.4175(c/a)$ is shown, the resonator has a quality factor around 1223.

3. Conclusion

We have presented the design of a surface mode ring resonator based on the dielectric PC. If the wavelength is 1550 nm at $f=0.41386$ (c/a), the lattice constant is 641.5 nm, so the radius of SMRW for $R=4a$ is about 2.5 μm. Compared with the other surface mode ring resonators [3], the calculated results demonstrated that the ring resonator have a lower radiation loss with a very smaller size because of the good wave-guiding of surface mode. The structure provides a possibility of channel drop filter, and can be used in future WDM optic communication systems.

Acknowledgments

This work was supported by the National Natural Science Foundation of China (Nos. 60978010, 60907032, and 60825103), the Natural Science Foundation of Zhejiang Province (No. Y1090169), the Foundation of Zhejiang University of Technology (No. 0901103012408), and the Open Fund of the State Key Laboratory of Advanced Optical Communication Systems and Networks, China(No. 2008sh07).

References

[1] S. Otto, SPIE 6872 (2008) 68720H.
[2] B. Wang, G.P. Wang, Appl. Phys. Lett. 89 (2006) 133106.
[3] XiaoSanshui , LiuLiu , QiuLiu , Opt. Express 14 (7) (2006) 2932.
[4] B.E. Little, S.T. Chu, H.A. Haus, J. Foresi, J.P. Laine, IEEE J. Lightwave Technol. 15 (1997) 998.
[5] T. Barwicz, M. Popovic, P. Rakich, M. Watts, H. Haus, E. Ippen, H. Smith, Opt. Express 12 (2004) 1437.
[6] Janne-Matti Heinola, Kimmo Tolsa, IEEE Trans. Dielec. Elec. Insul. 13 (4) (August 2006) 717.
[7] N.A. Yebo, D. Taillaert, J. Roels, D. Lahem, M. Debliquy, D. Van Thourhout, R. Baets, IEEE Photon. Technol. Lett. 21 (14) (July 15, 2009) 960.
[8] Zexuan Qiang, Weidong Zhou, Richard A. Soref, Opt. Express 15 (2007) 1823.
[9] Wei-Yu Chiu, Tai-Wei Huang, Wu. Yen-Hsiang, Yi-Jen Chan, Chia-Hunag Hou, Yi-Jen Chan, Chia-Hunag Hou, Huang Ta Chien, Chii-Chang Chen, Opt. Express 15 (2007) 15500.
[10] V. Dinesh Kumar, T. Srinivas, A. Selvarajan, Photon. Nanostr. 2 (3) (2004) 199.
[11] Seok-Hwan Jeong, Jun-ichiro Sugisaka, Noritsugu Yamamoto, Makoto Okano, Kazuhiro Komori, Jpn. J. Appl. Phys. 46 (2007) L534.
[12] Ma Max, Kazuhiko Qgusu, Jpn. J. Appl. Phys. 49 (2010) 052001.
[13] A.I. Rahachou, I.V. Zozoulenko, J. Opt. Soc. Am. B 23 (2006) 1679.
[14] A.Q. Liu, E.H. Khoo, T.H. Cheng, E.P. Li, J. Li, Appl. Phys. Lett. 92 (2008) 021119.
[15] Ziyang Zhang, Matteo Dainese, Lech Wosinski, Min Qiu, Opt. Express 16 (7) (2008) 4621.